It's all in the timing: vegetative phase change alters selection under drought and contributes to local adaptation

Erica H Lawrence-Paul[1]*, Jessica Janakiraman[1], Matthew R Lawrence-Paul[2], Rotem Ben-Zeev[1], Amanda Penn[1], Jesse R Lasky[1,3]

1Department of Biology
Pennsylvania State University
University Park, PA 16802
USA

2 Department of Cancer Biology
Perelman School of Medicine, University of Pennsylvania
Philadelphia, PA 19131
USA

3 PAC Herbarium
Pennsylvania State University
University Park, PA 16802
USA

*email: lawrence.erica.h@gmail.com

Abstract

The timing of developmental transitions is critical for environmental adaptation, allowing organisms to align stress tolerant and sensitive stages with harsh and benign periods, respectively. This timing across seasons (i.e. phenology) is often under spatially-varying selection across climate gradients, and species often exhibit genetic clines in phenology. Clines for transitions like germination and flowering time are well documented; less is known about the juvenile-to-adult vegetative phase change (VPC) – a conserved (among plants) yet visually subtle developmental transition marked by changes in leaf morphology and physiology. Alternatively, developmental tradeoffs can reduce fitness differences between genotypes and promote diversity within populations. Here, we tested 158 diverse genotypes of *Arabidopsis thaliana* under drought during either the juvenile or adult vegetative phases along with well-watered controls. We measured performance, physiology, and timing of developmental transitions. We found strong rank-changing genotype-environment interactions with fitness depending on the stage at which drought occurred, indicating tradeoffs and distinct mechanisms

of drought adaptation between different stages. Fitness reductions were generally greater under juvenile drought, suggesting that the juvenile phase is more vulnerable than the adult phase to stress. Adult plants significantly increased water use efficiency in response to drought but juvenile plants did not, consistent with earlier results showing reduced plasticity in the juvenile phase. Genome-wide association mapping revealed candidate loci for the timing of VPC and stage-specific drought responses. Globally, VPC timing was weakly related to climate but in Iberia there was a significant trend of early VPC in seasonally dry climates and late VPC in moist climates. Analysis of global geographic variation in putative QTL showed a strong depletion in SNPs associated with the timing of VPC and juvenile drought fitness, suggesting variation in these loci is maintained within populations due to consistent tradeoffs all across *Arabidopsis* range. These results demonstrate that the timing of VPC contributes to adaptive responses to drought and that tradeoffs across developmental stages help maintain genetic diversity in natural populations.

Introduction

The timing of developmental transitions is critical for organismal adaptation. As organisms transition through developmental phases their morphology and physiology changes, altering the way they respond to environmental stress. Understanding the regulation of developmental timing as well as how distinct developmental phases modulate physiology is essential for predicting how organisms will respond to changing climates and for identifying genes and traits important for stress tolerance across lifespans (Lawrence-Paul & Lasky, 2024).

Developmental timing is especially important in plant adaptation. Flowering time and germination are well known contributors to local adaptation. Early flowering time is often favored in environments with terminal drought or shorter growing seasons as part of a “drought escape” strategy (Kenney *et al.*, 2014; Austen *et al.*, 2017). The timing of germination impacts local adaptation both through its effects on flowering time (Korves *et al.*, 2007; Burghardt *et al.*, 2015) as well as a plants ability to survive and accumulate biomass prior to reproduction (Donohue, 2002). The timing of these developmental transitions dictates the organs exposed to specific environmental conditions and the environment the plant will experience when it shifts resources from producing vegetative to reproductive structures. While there is an abundance of evidence that the timing of developmental transitions is important for plant adaptation, the transition between juvenile and adult vegetative phases of development, vegetative phase change (VPC), has not been well studied in this context.

Phenotypes exhibited at one developmental stage may influence or constrain phenotypes at another stage. Many traits increase fitness at one stage at the expense of fitness at another stage, creating a fitness tradeoff across development (Stearns 1989). When these tradeoffs balance, variation in the underlying traits is neutral and this variation will not be eliminated by selection (Mojica *et al.*, 2012). Plants are classic systems for tradeoffs across development (Bazzaz *et al.*, 1987; Young & Augspurger, 1991; Lundgren & Marais, 2020), but whether these tradeoffs involve VPC is not well documented.

79 Vegetative phase change is regulated by a highly conserved microRNA, miR156, and its
80 targets, *SQUAMOSA PROMOTER BINDING-LIKE* (*SPL*) transcription factors (Wu & Poethig,
81 2006; Willmann & Poethig, 2007; Wu *et al.*, 2009). In *Arabidopsis,* there are 16 *SPL* genes, 10
82 of which are targets of miR156, with roles in regulating shoot growth and morphology, root
83 development, floral induction, stress responses, and more (Xu *et al.*, 2016). As plants transition
84 from juvenile to adult phases, they undergo morphological and physiological changes that
85 influence environmental interactions and resource use. For example, in *Populus*, *Zea mays* and
86 *Arabidopsis,* juvenile leaves have a "fast" carbon economic strategy, characterized by low
87 construction costs, while adult leaves have higher construction costs, longer lifespans and
88 higher return on investment (Lawrence *et al.*, 2022). These ontogenetic shifts result in distinct
89 ecophysiological strategies with juvenile typically having higher photosynthetic rates in low-light
90 environments and responding more quickly to sunflecks, making them better suited for shaded
91 canopy environments. In contrast, adult leaves have greater maximum photosynthetic capacity
92 under high light. Physiological differences between juvenile and adult phases also influence
93 stress responses. In tomato, miR156 overexpression alters abscisic acid (ABA) sensitivity,
94 causing stomata to close more slowly in response to drought (Visentin *et al.*, 2020). These
95 ontogenetic differences support the idea that selection on the timing of vegetative phase could
96 facilitate local adaptation. In *Eucalyptus*, which exhibits a visually striking shift in juvenile and
97 adult leaf morphology, coastal populations experiencing greater salt and drought stress appear
98 to be selected for earlier VPC compared to inland populations (Hudson *et al.*, 2014). Later
99 studies revealed that juvenile leaves had more vulnerable xylem, making them more susceptible
100 to drought damage than adult leaves, further supporting the adaptive value of early VPC in
101 stressful environments (Lucani *et al.*, 2019).
102 In addition to selection on the timing of VPC, environmental stress at different periods of
103 development could alter selection on genes and traits during each developmental phase.
104 Because development controls the expression of traits, development may also influence the

evolution of mutations controlling those traits. For example, we have shown that juvenile leaves are more canalized and less plastic in response to abiotic stress compared to adult leaves in *Arabidopsis* (Lawrence-Paul *et al.*, 2023). As a result, adaptation to environmental conditions early in life may involve mutations that affect constitutive trait expression, while adaptation to environmental conditions experienced at the adult stage may involve mutations affecting plasticity. Some support for this hypothesis is found in the role that miR156 plays in suppressing SPLs in the juvenile stage while these SPLs can act as positive regulators of abiotic stress responses (Mao *et al.*, 2016; Xu *et al.*, 2016; Zhao *et al.*, 2024). Therefore, mutations affecting stress responsive expression of genes partly regulated by SPLs may only manifest phenotypes in adult plants experiencing those stressors. The evolution of expression plasticity likely plays an important role in local adaptation to climate in *Arabidopsis* (Lasky *et al.*, 2014; Lee *et al.*, 2024), however we hypothesize that this GxE is weaker and weakly associated with performance at the juvenile stage.

Due to the little knowledge of natural variation in the timing of VPC (Foerster *et al.*, 2015; Doody *et al.*, 2022; Wang *et al.*, 2024) and few studies that examine plant stress response during these phases of development (Lawrence-Paul *et al.*, 2023), we have little information on how the timing of VPC contributes to local adaptation and phase-specific responses to abiotic stress. Here we investigate how natural variation in the timing of VPC and phase-specific responses to drought contribute to local adaptation. We used growth chamber common gardens with drought treatments applied at different stages to *Arabidopsis thaliana* natural genotypes to ask the following questions:

1. Is adaptation to drought stage-specific or are drought adapted genotypes more fit under drought at any stage? Are there tradeoffs in adaptation to drought at one stage versus another stage?

2. Are the same genes associated with drought response across developmental phases or are they phase-specific?
3. How does natural variation in VPC timing contribute to drought adaptation?

Methods

Plant Material

Seeds of 158 *Arabidopsis thaliana* natural accessions (Table S1) were obtained from the *Arabidopsis* biological resource center and grown for seed bulking in a Conviron walk-in growth chamber with 16-hour days at 22°C and 8-hour nights at 18°C with light provided by Philips 32 Watt, 6500K and 4100K fluorescent bulbs and Euri A21 2700K LED bulbs with an average PAR of 194 µmol m^2 s^{-1}, and 65% relative humidity. Seeds were stratified in 800 ppm Gibberellic acid at 4ºC for 5 days then planted in 2 ¼ inch pots filled with Pro-Mix BX growing mix. Pots were covered with humidity domes until after germination and pots were bottom watered regularly to maintain moisture. The natural accessions used were chosen as a subset from those used in Exposito-Alonso *et* al. 2018, where accessions were selected from the 1001 genomes project based on sequence quality and geographic distribution.

Plant Growth Conditions

For experimental plants, seeds collected from the bulking were stratified for 5 days as described above and planted in 2 ¼ inch pots filled with a 1:2 sand (Quikrete), BX potting mix (Pro-mix) mix with thin layer of 100% BX potting mix on top. The 60/30 mix was used for faster drainage so that drought conditions were met quickly when water was withheld, while the layer of 100% BX was used to aid in seed germination and image analysis. Potting substrate was supplemented with 2x miracle grow and marathon granules for added nutrients and pest management. Plants were grown in a Conviron chamber with environmental conditions as

155 described above. Plants were well-watered for 10 days before being moved to a cold room at
156 4°C for a 5-week vernalization. Plants used in experiments for validating GWAS results did not
157 undergo a vernalization treatment and lacked the layer of 100% BX.
158
159 *Drought treatments*
160 Well-watered plants were bottom watered twice daily, 12 hours apart, for 10 mins using
161 an automated watering system comprised of flood trays, water reservoirs, and water pumps on
162 timers. Plants in the juvenile drought treatment experienced a 10-day drought starting 47 days
163 after planting (2 days after being moved back to growth conditions following vernalization).
164 During the drought, plants were bottom watered for 10 mins every 84 hours. The timing of adult
165 drought treatments was determined based on flowering time during the bulking for each
166 genotype to ensure plants began drought prior to flowering but after transitioning to the adult
167 vegetative phase. Accessions were binned into four groups of 40 based on flowering time,
168 accessions in group 1 began adult drought treatments 55 days after planting, group 2, 60 days
169 after planting and groups 3 and 4, 65 days after planting (Table S1). Adult drought treatments
170 were conducted the same way as juvenile drought treatments for 10-days with watering
171 intervals of 84 hours. Following drought treatments, all plants returned to well-watered
172 conditions with a watering interval of 12 hours.
173 Plants used in experiments for validating GWAS results experiments were well-watered
174 by bottom watering for 10 mins once a day. During drought treatments, water was withheld for 7
175 days. Juvenile drought began when the first two true leaves were visible, and adult drought
176 began when leaf 5 was visible. Following drought treatments, all plants returned to well-watered
177 conditions with a watering interval of once per day. Volumetric water content of growth media
178 was measured hourly with METER Group EC-5 sensors.
179
180 *Phenotyping for the timing of vegetative phase change*

181 We used the first leaf with abaxial trichomes as a marker for the onset of vegetative
182 phase change (Telfer *et al.*, 1997; Willmann & Poethig, 2011). A minimum of 3 replicates per
183 genotype were measured for all natural accessions in the well-watered conditions and a subset
184 of 30 genotypes were measured in the juvenile drought treatment to look at plasticity in the
185 timing of VPC. Daily images taken of the rosettes by RaspberryPis were used to convert the
186 timing of VPC from leaf number to days by noting the date when the first leaf with abaxial
187 trichomes was visible.
188
189 *Phenotyping for rosette growth*
190 To study rosette growth responses to drought we measured rosette diameter on the first
191 and last day of drought treatments, and the corresponding days for well-watered control plants.
192 Measurements were taken with a combination of PlantCV (Gehan *et al.*, 2017) using the
193 "*Arabidopsis* multi-plant workflow" and threshold settings between 110-120 and manual
194 measurements in FIJI (Schindelin *et al.*, 2012). Change in size during drought was calculated by
195 subtracting the starting diameter from the final diameter.
196
197 *Phenotyping for fruit production*
198 Plants were harvested when the first fruit became mature determined by a yellowing in
199 color as Boyes *et al.*, 2001 determined that flowering is complete around the same day the first
200 silique shatters in Col-0. Shoots were cut at the soil surface and Inflorescences and rosettes
201 were separated and laid flat on black fabric and imaged with a Nikon D3200. Images were
202 analyzed for estimating fruit count following Vasseur *et al.*, 2018. We found the Vasseur model
203 predicted fruit count from images in our experiment well, with an R^2 of 0.91 for the linear
204 regression model (manual ~ predicted) between predicted versus manually counted fruits.
205

206 *Isotope discrimination analysis*

207 Plants for isotope analysis were grown as previously described. The two newest fully
208 expanded leaves for three replicates of each genotype were sampled at the end of the juvenile
209 drought treatment, the end of the adult drought treatment, and at corresponding time points for
210 well-watered controls. Leaf tissue was dried at 60°C for a minimum of 48 hours, then pooled by
211 genotype and treatment. Samples were ground to a fine homogenous powder using a
212 Benchmark Bead Bug 6 Microtube Homogenizer with a 1.6 mm stainless steel ball. Between
213 0.09 and 3.1 mg (typically ~2mg per sample) were weighed into 8 x 5 mm tin capsules using a
214 Sartorius MCE3.6P microbalance. Carbon and nitrogen isotope ratios and percent composition
215 were measured by the Cornell University Stable Isotope Lab using a Thermo Delta V isotope
216 ratio mass spectrometer (IRMS) interfaced to a NC2500 elemental analyzer. The primary
217 reference scale used for δN was atmospheric air and for δC was Vienna Pee Dee Belemnite.
218

219 *Bioclimatic associations with the timing of VPC*

220 Bioclimatic variables corresponding to the latitude and longitude of each accession's
221 origin were obtained from WorldClim version 2.1 (Fick & Hijmans, 2017) at a spatial resolution
222 of 2.5 arc-minutes. We used linear regression to look for correlations between the bioclimatic
223 variables and the timing of VPC. Analyses were conducted both globally, across all accessions,
224 and within regions. Given the wide variation in both climate and VPC timing among accessions
225 from the Iberian Peninsula (Spain and Portugal), and the fact that clines often change between
226 parts of the *Arabidopsis* range (Gamba *et al.*, 2024). We performed additional analyses on this
227 subset to explore region-specific patterns.
228

229 *Genome wide association analysis*

230 Genome wide association studies (GWAS) were conducted using the GWA-Portal tool
231 (Seren 2018) with the Accelerated Mixed Model (AMM) protocol and 1001 Fullsequence dataset
232 (TAIR9). GWAS was performed separately for each trait, using mean trait values per genotype.
233 The datasets included 158 *Arabidopsis* accessions with genotype and phenotype data. A minor
234 allele frequency (MAF) threshold of 0.05 was applied. Candidate genes near the top SNPs were
235 identified using Araport11 annotations and the TAIR Gene Search tool (arabidopsis.org)
236 examining a 100 kb window around each SNP.
237
238 *Statistical Analyses*
239 All statistical analyses were performed in R version 4.1.0 (R Core Team, 2021) or JMP
240 Pro 18. Figures were generated using the ggplot2 package in R. Phenotypic differences across
241 control, juvenile and adult drought treatments were assessed using analysis of variance
242 (ANOVA) followed by Tukey's post hoc test. Comparisons of isotope discrimination between
243 drought treated and corresponding well-watered control plants were conducted using Student's
244 T-test. Correlations between continuous variables were evaluated using linear regression
245 models (R function lm).
246
247 *Tests of selection on top GWAS SNPs*
248 If genetic loci are under spatially varying selection, we expect they will exhibit greater
249 spatial variation in allele frequency than the genomic background. By contrast, loci under
250 balancing or contributing to traits under consistent stabilizing selection may show less spatial
251 variation than the genomic background. We tested for this pattern across a range of spatial
252 scales using published calculations of scale-specific genetic variance across the native
253 accessions in the 1001 Genomes panel (Lasky *et al.*, 2024). We took either the top 100 or 1,000
254 SNPs from GWAS for timing of VPC and fitness in each drought treatment and asked if the

mean variance at a range of spatial scales was greater or less than expected from 100 permutations of SNP labels around the genome (Lasky *et al.*, 2024).

Results

Natural variation in the timing of vegetative phase change

We observed substantial variation in the timing of vegetative phase change (VPC) across the 158 *Arabidopsis* accessions, with transitions as early as leaf 3 or day 48 and as late as leaf 19 or day 64 (Figs. 1, S1). Interestingly, there were no clear geographic patterns in the distribution of VPC timing, suggesting that this diversity is maintained within regions (see analyses below). Two measures of VPC timing, the first leaf with abaxial trichomes, and the number of days from planting until that leaf was visible, were strongly correlated ($p = 1.6e^{-25}$, $R^2 = 0.51$; Fig. S1) suggesting little variation in leaf initiation rate during the juvenile phase. The two morphological indicators of VPC, abaxial trichomes and leaf serrations, were also significantly correlated ($p = 1.2e^{-10}$, $R^2 = 0.24$; Fig S1), although some independent variation was evident. This is consistent with previous work that shows the onset of adult traits is staggered due to differential regulation by SPL transcription factors, and varying sensitivity of different SPL genes to miR156 levels (Xu *et al.*, 2016; He *et al.*, 2018).

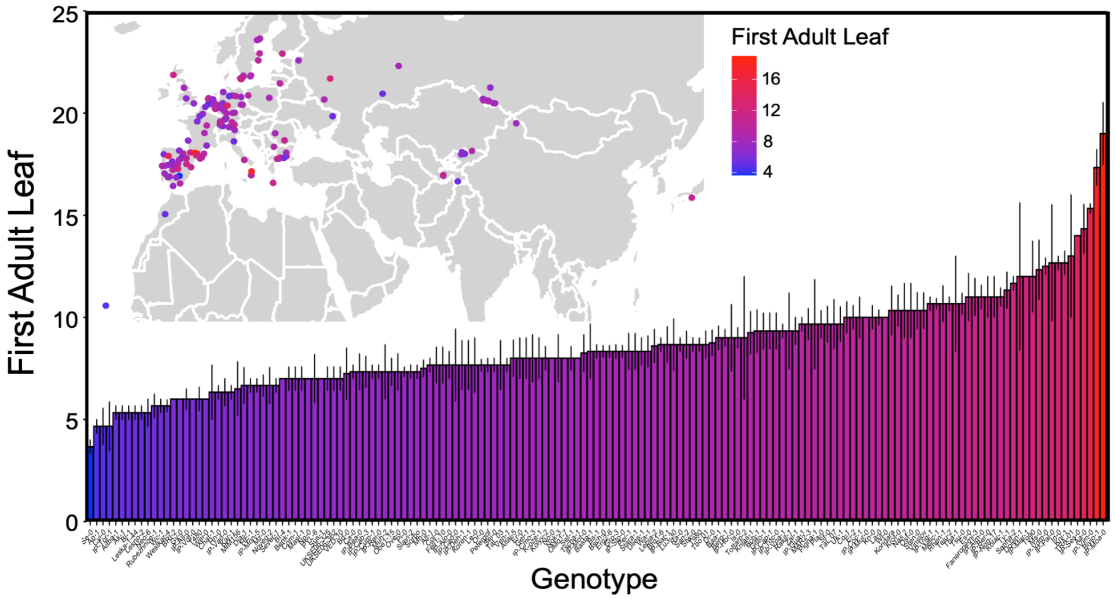

Figure 1. Natural variation in the timing of vegetative phase change (VPC). Timing of VPC based on the first adult leaf with abaxial trichomes for 158 natural accessions used in this study. Accessions are plotted on the map in the location where they originated from, and points are colored based on first adult leaf. Bars represent the mean ± SE for a minimum of 3 replicates per genotype.

The time spent in each developmental phase is not correlated

We found that the duration of each developmental phase – juvenile vegetative, adult vegetative, and reproductive (time between flower opening and fruit maturation) – was not significantly correlated (juvenile vs adult: $p = 0.042$, $R^2 = 0.027$; juvenile vs reproductive: $p = 0.98$, $R^2 = 4.8e^{-6}$; adult vs reproductive: $p = 0.34$, $R^2 = 0.0061$; Figs. 2, S2). This indicates that genotypes that transition to the adult phase earlier may compensate by spending more time in the adult vegetative phase, ultimately reaching reproductive maturity on a similar timescale as genotypes with a slower juvenile transition. For example, Ak-1 spends an average of 13.3 days in the juvenile phase, 16.3 days in the adult phase, and 19.3 days in the reproductive phase for a total of 48.9 days from planting to fruit maturation. In contrast, Giffo-0 spends 26.5 days in the juvenile phase, but has a shorter 11.2 day adult phase and 15.3 day reproductive phase, totaling 53 days. Despite different developmental trajectories, both genotypes complete their life cycle in a similar timeframe.

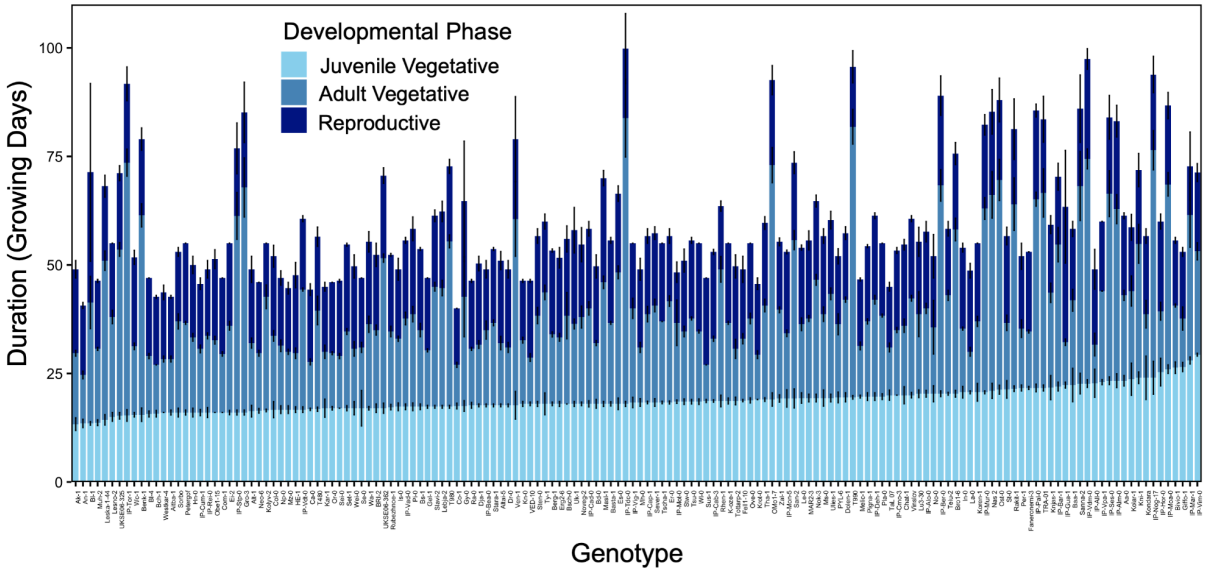

Figure 2. Time spent during juvenile, adult, and reproductive developmental phases for 158 accessions of *Arabidopsis thaliana*. Bars represent mean ± SE for the duration in days spent in each phase. Juvenile phase, in light blue, is defined as the time between planting and appearance of first adult leaf (excluding the 35 days spent at 4℃ for vernalization), adult phase, in medium blue is defined as the time between the appearance of the first adult leaf and first open flower, and reproductive (dark blue) is defined as the time between first open flower and first mature fruit.

Plasticity in the timing of VPC in response to drought

The timing of VPC showed limited plasticity in response to drought. When abaxial trichomes were used as a marker of VPC, some genotypes showed accelerated transition while others were delayed, however the genotype-by-environment (GxE) interaction was not significant (ANOVA genotype x treatment interaction $p = 0.47$; Fig 3A). On average, plants transitioned at a similar leaf number in both treatments. The first adult leaf appeared at leaf 8.79 in control and leaf 8.97 in the juvenile drought treatment (ANOVA treatment $p = 0.49$). Using leaf serrations as a marker led to similar results for GxE (ANOVA GxE $p = 0.16$; Fig. 3B). However, the overall shift in VPC timing assessed using serrations was slightly delayed under drought, with a mean transition at leaf 7.19 in control and 7.64 in juvenile drought, and this difference was statistically significant ($p = 0.02$). Overall, the limited plasticity in the timing of

310 VPC in response to our drought treatment is reflected in strong correlations between control and
311 drought treatments for both markers (linear regression: trichomes p = 6e-05, R2 = 0.46;
312 serrations p =0.001, R2 = 0.33, respectively; Fig S3).
313

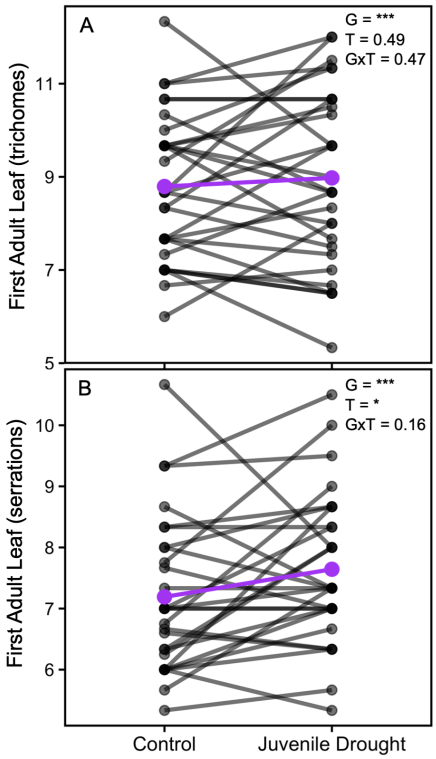

314
315
316 **Figure 3.** Plasticity in the timing of vegetative phase change between well-watered control and juvenile
317 drought treatments. Black circles represent the mean first adult leaf based on abaxial trichomes (A) or
318 serrations (B) for each of the 30 accessions examined in both treatments connected between treatments
319 by a black line. Purple circles and lines represent the mean for all genotypes. ANOVA results depicted in
320 the top right corner of each plot with *** and * indicating p < 0.001 and 0.05 respectively.
321
322 *Flowering time depends on developmental phase when drought occurs*

323 The majority of genotypes delayed flowering in response to drought during either the
324 juvenile or adult phase, 77% and 79% respectively (ANOVA: p < 0.001 for both drought
325 treatments, Fig. 4A-B). Under juvenile drought, flowering was delayed by as much as 40.9 days
326 (Tra-01), while some genotypes like Gy-0, flowered as much as 6.6 days earlier than under well-
327 watered control conditions. In the adult drought treatment, shifts in flowering time were even
328 greater for some genotypes with the largest delay of 55.8 days (Sanna-2) and the greatest

acceleration of 15.9 days (Ven-1). Significant genotype and genotype-by-treatment effects were detected in both phases (ANOVA G: $p < 0.001$, GxT: $p < 0.001$).

Responses to drought varied depending on the developmental phase during which it occurred. For example, Sanna-2 showed little change in flowering time under juvenile drought (3.8-day delay) but a strong delay under adult drought (55.8-day delay), resulting in a 52-day difference in flowering time between drought treatments. In contrast, Ost-0 exhibited minimal response under adult drought (0.5-day delay), but a substantial delay under juvenile drought (37.4 days), leading to a 37-day flowering time difference. The significant GxT interaction across all genotypes (ANOVA GxT: p <0.001, Fig. 4C) indicates that both the occurrence of drought and the developmental phase during which it is experienced play critical roles in determining flowering time.

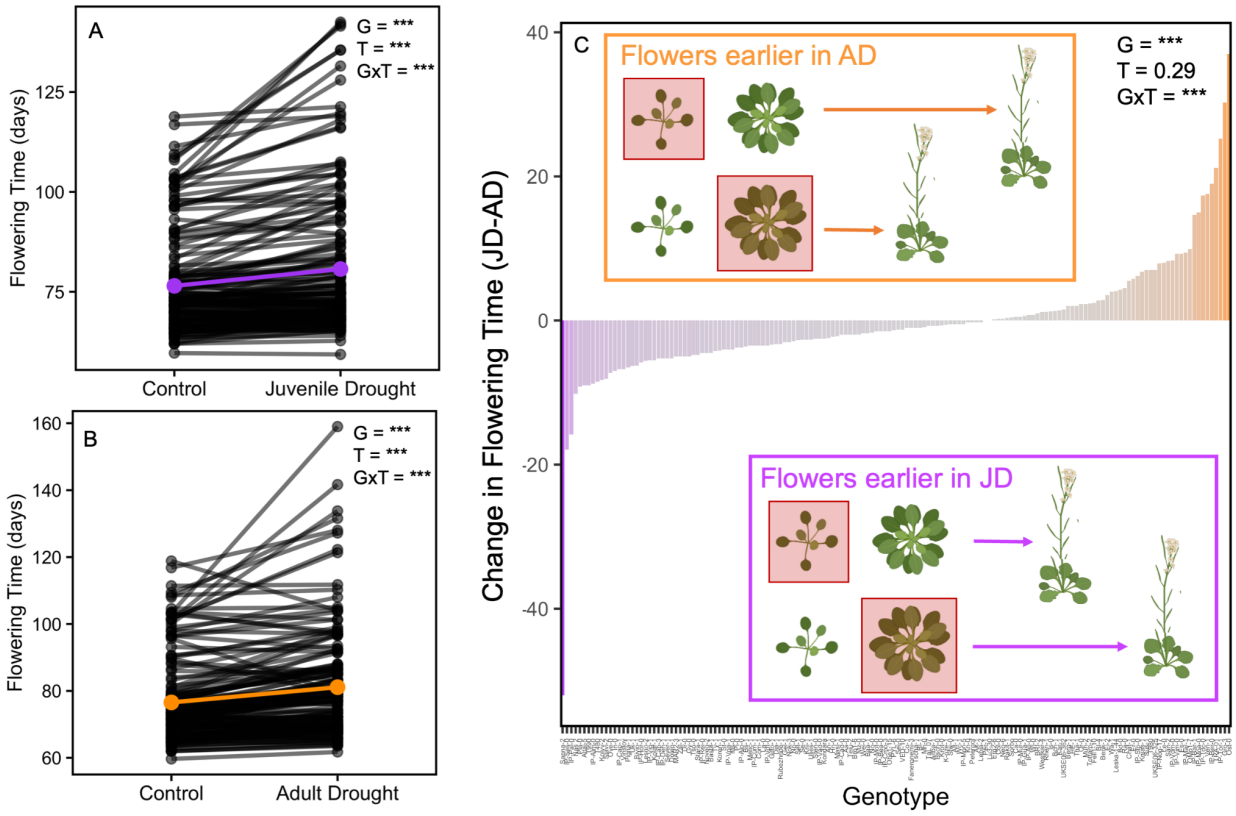

Figure 4. Flowering time responses to drought depend on the developmental phase when drought occurs. Black circles represent the mean flowering time for each of 158 accessions of *Arabidopsis thaliana* in well-watered control and juvenile (A) or adult (B) drought environments. Black lines connect means for each genotype. Purple circles and lines represent the mean across all genotypes between control and juvenile drought treatments. Orange circles and lines represent the mean across all genotypes between control and adult drought treatments. The change in flowering time between drought treatments (-C) for each accession is represented as bars with purple bars indicting plants flowered earlier in the juvenile drought treatment compared to adult drought (flowering time in juvenile drought - adult drought < 0) and orange bars indicting plants flowered earlier in the adult drought treatment compared to juvenile drought (flowering time in juvenile drought - adult drought > 0). ANOVA results are depicted in the top right corner of each plot.

The developmental phase when a plant encounters drought alters fitness effects

Both drought treatments resulted in a significant reduction in fruit production compared to well-watered controls (ANOVA treatment effect: juvenile drought vs. control $p < 0.001$, adult drought vs. control $p < 0.01$, Fig. 5A-B). On average, plants produced fewer fruits when drought occurred during the juvenile phase than during the adult phase (ANOVA treatment $p <0.001$, Fig. 5C). However, a significant genotype-by-environment interaction ($p < 0.001$) revealed that this pattern was not consistent across genotypes. Weak correlations between fruits produced in each treatment further support genotypic variation in fitness responses to drought (linear regression for fruits produced in control vs juvenile drought $R^2 = 0.08$, control vs adult drought $R^2 = 0.06$, juvenile drought vs adult drought $R^2 = 0.1$, Fig. S4).

For example, Aa-0 (Fig. 5C, blue line) produced an average of 84 fruits under juvenile drought but only 30 fruits under adult drought, dropping in fitness rank from 12th to 153rd. In contrast, Ove-0 (Fig. 5C, red line) produced 208 fruits under adult drought but only 43 fruits under juvenile drought, falling from 1st to 90th in rank. Some genotypes such as Krot-0 (Fig. 5C, purple line), showed relatively stable performance, producing 147 fruits in juvenile drought and 138 fruits in adult drought. Still, even for such genotypes, the rank order shifted due to more pronounced phase-specific responses in others, causing Krot-0 to drop from 2nd in the juvenile drought to 56 in adult drought treatment.

These results demonstrate that the developmental timing of drought stress alters its fitness consequences. Shifts in genotype performance and rank order across treatments

375 suggest that the phase in which drought occurs can shape selection and pressures in natural

376 populations.

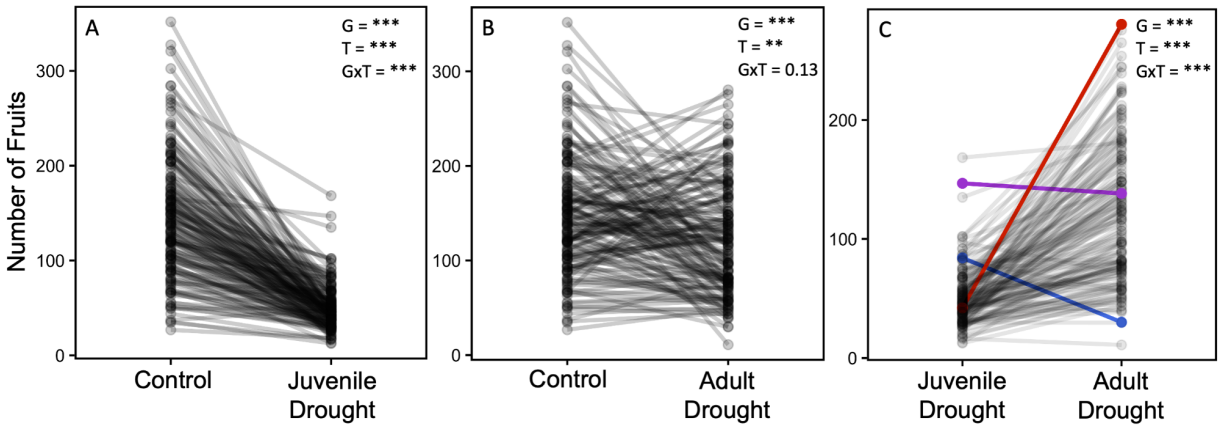

377
378
379 **Figure 5.** Drought effects on fitness depend on the developmental phase when drought occurs. Black
380 circles indicate the mean number of fruits produced in well-watered control, juvenile drought or adult
381 drought treatments and lines connect means between treatments. Genotypes with different phase-
382 specific drought responses highlighted in panel C, red = Ove-0, purple = Krot-0 and blue = Aa-0. ANOVA
383 results displayed in the top right corner of each plot where *** and ** indicate $p < 0.001$ and 0.01
384 respectively.
385
386 *Drought mediated shifts in water use efficiency (WUE) depend on developmental stage*

387 Using carbon isotope composition ($\delta^{13}C$) as a proxy for water use efficiency (WUE), we

388 found that drought affected WUE differently depending on the plant's developmental stage. In

389 the juvenile phase, WUE did not change significantly in response to drought (p = 0.16), whereas

390 in the adult phase, drought led to a significant increase in WUE (p <0.0001; Fig. 6). The median

391 $\delta^{13}C$ increased by only 0.11‰ between well-watered and drought-stressed plants in the juvenile

392 phase, compared to an increase of 0.84‰ in the adult phase.

393 Variation in WUE among genotypes was also greater in the adult phase. The

394 interquartile range (IQR) of $\delta^{13}C$ values was 1.29‰ and 1.58‰ for adult control and drought

395 treatments respectively, compared to 0.95‰ and 0.875‰ in juvenile control and drought

treatments. This suggests greater plasticity and greater genetic variation in WUE during the adult phase.

We observed significant but weak negative correlations between WUE and fruit production under drought, indicating that genotypes with higher WUE tended to produce fewer fruits (juvenile drought p =0.02, R^2=0.035; adult drought p =0.0018, R^2 = 0.062). This trade-off may reflect a cost of increased WUE to carbon assimilation, potentially adaptive if drought were extreme enough to cause mortality of low WUE genotypes.

There were also weak but significant correlations between WUE and number of juvenile leaves across several conditions. Genotypes that transitioned earlier to the adult phase tended to have lower WUE (juvenile control: p = 0.03, R^2 = 0.031; adult control: p < 0.001, R^2 = 0.07; adult drought: p < 0.001, R^2 = 0.082). However, this relationship was absent under juvenile drought stress (p = 0.13, R^2 = 0.015).

Overall, these results show that developmental stage mediates both the magnitude and variability of WUE responses to drought, with greater plasticity and stronger associations with other traits observed during the adult phase.

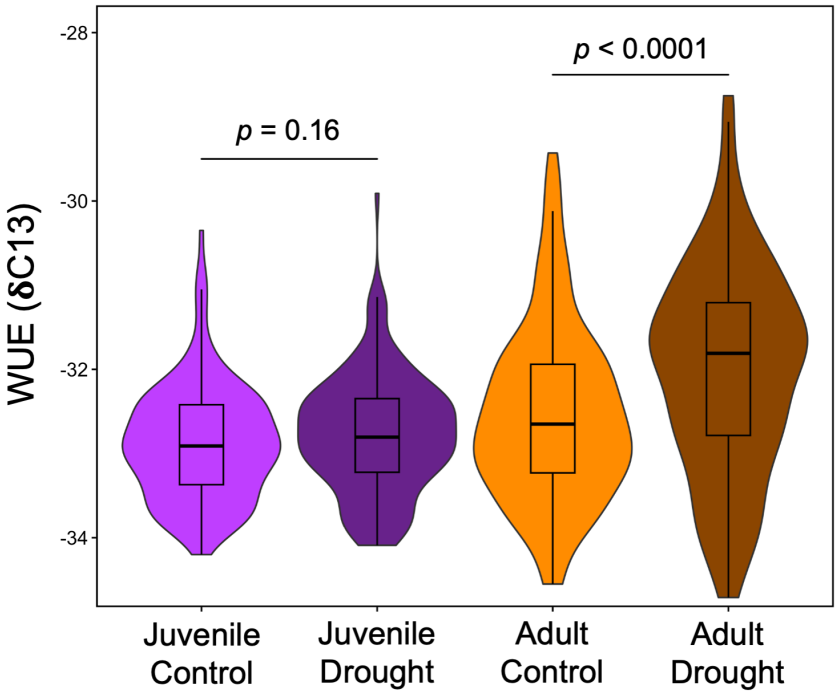

Figure 6. Carbon isotope discrimination shows phase-specific responses of water use efficiency (WUE) to drought. Box plots display the median and interquartile range for $\delta^{13}C$ from leaf tissue collected at the end of the juvenile drought period from plants in well-watered control (light purple) or drought (dark purple) treatments and at the end of the adult drought period from plants in well-watered control (light orange) or drought (dark orange) treatments. Violin plots show the distribution of the data for all 158 genotypes with thick sections indicating higher frequency and thinner sections lower frequency values. Results from Student's t-test between control and drought treatments at each developmental phase shown above each comparison.

The timing of VPC is associated with local precipitation

Globally, the timing of VPC showed a significant but weak positive association with precipitation in each genotype's native environment ($p < 0.05$, $R^2 = 0.0125$; Fig. 7A). However, this relationship was much stronger within Iberian populations ($p < 0.001$, $R^2 = 0.32$; Fig. 7B), which span a broad range of climatic conditions. In this region, genotypes from drier environments tended to undergo VPC earlier, potentially shifting from the more drought-sensitive juvenile phase to the more tolerant adult phase sooner. These patterns suggest that

429 natural selection may favor earlier VPC in environments with lower precipitation, aligning the

430 drought-tolerant developmental stage with periods of increased water stress.

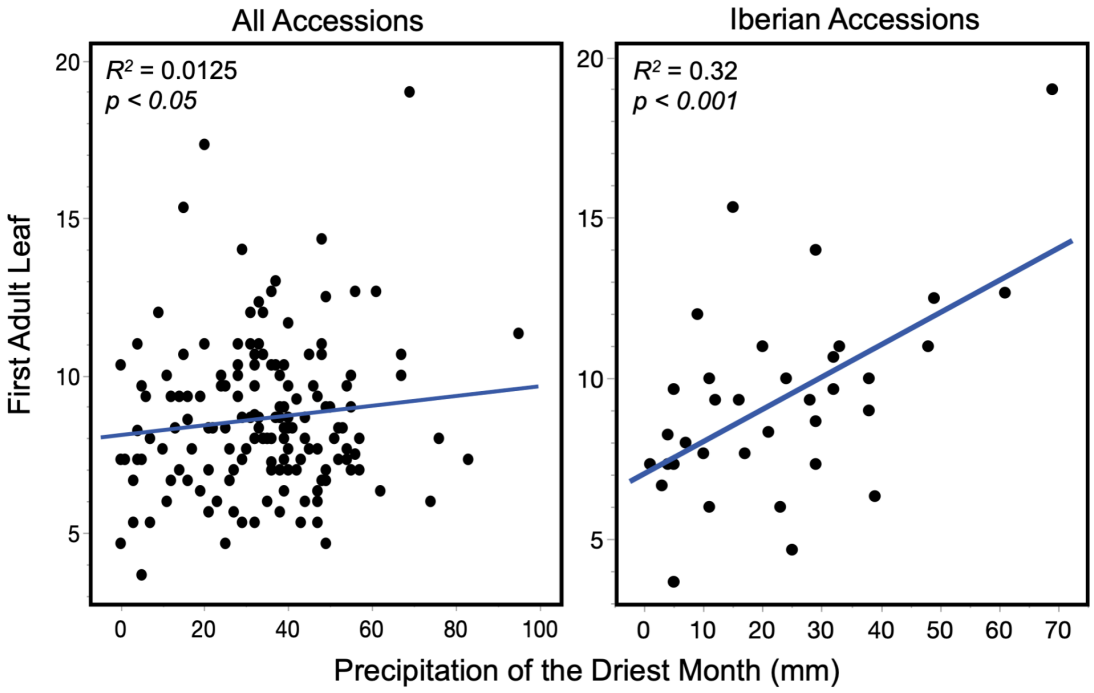

431 **Figure 7.** The timing of vegetative phase change is associated with precipitation in native climate.
432 Relationships between the timing of vegetative phase change measured as first leaf with abaxial
433 trichomes and precipitation of the driest month in home environment for all 158 accessions of *Arabidopsis*
434 *thaliana* used in this study (left) or only accessions from the Iberian peninsula (right). Blue lines represent
435 the least-squares regression line (all accessions: Y = 8.1 + 0.015X, Iberian accessions: Y = 7.03 + 0.1X)
436 and results from linear regression analysis displayed in the top left corner of each plot.
437

438 *GWAS identifies novel candidate genes for the timing of VPC and phase-specific regulators of*

439 *drought response*

440 We conducted separate genome-wide association studies (GWAS) to identify candidate

441 genes associated with natural variation in the timing of VPC, as well as fitness responses to

442 drought during the juvenile and adult phases (Fig. 8). As expected for complex polygenic traits,

443 no single nucleotide polymorphisms (SNPs) surpassed the significance threshold after

444 Bonferroni correction. Therefore, we focused on the SNPs with the lowest p-values for each

445 trait, recognizing these as potentially information loci for further investigation.

446 For the timing of VPC, measured as the first leaf with abaxial trichomes, we identified
447 candidate genes nearest the top-associated SNPs. Notably, several candidates selected are
448 associated with the miR156-SPL regulatory pathway. These include *CYP71B14* (AT5G25180)
449 previously described as a target of *AGL15*, which regulates miR156 expression, and *ESE3*
450 (AT5G25190), an AP2/ERF transcription factor family member with shared targets of SPL
451 genes. Additional candidate genes are involved in cell development, gene silencing and
452 microRNA biogenesis such as *SMR8* (AT1G10690), *CLASSY3* (AT1G05490) and *PRL2*
453 (AT3G05350), respectively.
454 To identify loci associated with drought response, we used the $\log_2$-fold change in fruits
455 produced under relative to well-watered control conditions. Distinct sets of genes were
456 associated with drought tolerance depending on whether the drought occurred during the
457 juvenile or adult phase, suggesting phase-specific genetic architecture of drought response.
458 Candidate genes near top SNPs in the juvenile phase included *P4P5K* (AT1G60270), *EXLRR10*
459 (AT3G25670), and *BPC6* (AT5G42520), all previously implicated in abiotic stress responses. In
460 the adult phase, candidates included *PROSCOOP2* (AT5G44567), *DREB2* (AT2G40350), and
461 *GALT4* (ATG27120) which have documented roles in drought or stress signaling. Additional
462 genes, such as *PUB19* (AT1G60190), *ADP1MA1* (AT1G10730), and *ARA1* (AT2G40350), are
463 involved in ABA signaling, starch biosynthesis, and trafficking to vacuoles respectively, further
464 supporting their potential roles in phase-specific drought adaptation.
465
466

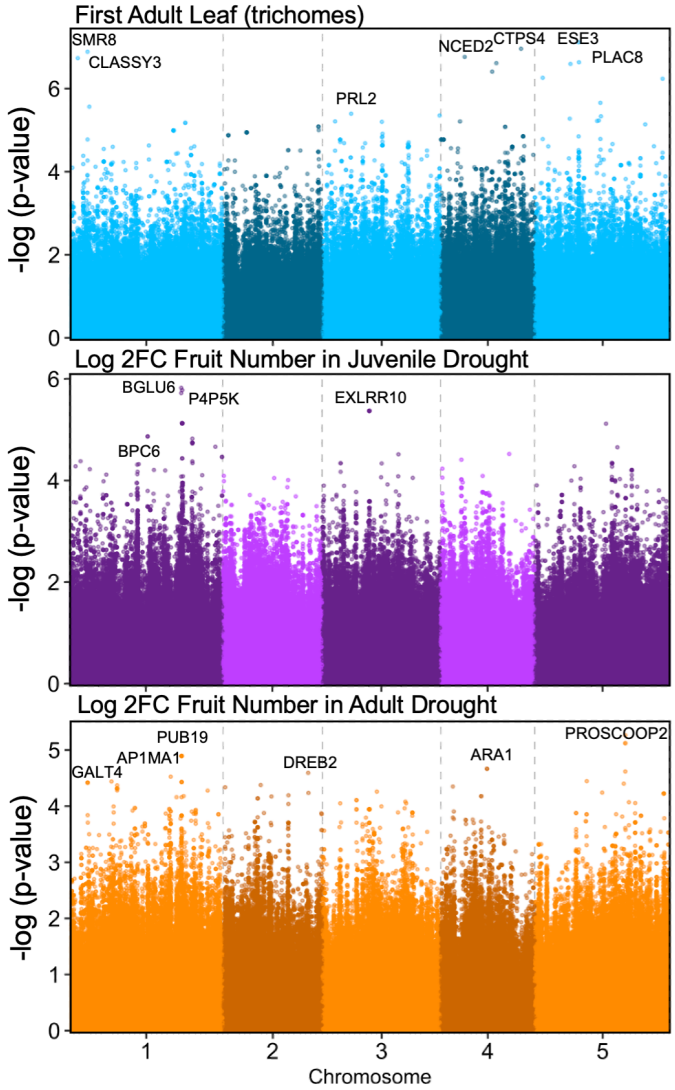

Figure 8. Manhattan plots of genome wide association analysis on timing of vegetative phase change and fitness responses to drought during juvenile and adult phases of development. Manhattan plots show the association of each SNP with the first leaf with abaxial trichomes (blue), the $\log_2$ fold-change in fruits produced between well-watered control and juvenile drought (purple) or adult drought (orange) treatments. Annotations indicate genes associated with top SNPs used in further analysis.

Evidence of selection on GWAS SNPsthese genes

We found that the top SNPs for the timing of VPC and fruit number under juvenile drought had much less geographic variation than expected across a range of spatial scales. Specifically, the timing of VPC based on trichomes top 1000 GWAS SNPs had significantly low spatial variation at the largest scale tested, 2980 km (two tailed permutation test, $p < 0.02$). Additionally, the top 1000 and top 100 SNPs for juvenile fruit number had significantly low

481 spatial variation at this scale (p = 0.04 in both cases), and the top 1000 SNPs had low spatial
482 variation at the ~1360 and ~620 km scales (p <0.02 and p = 0.04, respectively). By contrast,
483 adult fruit number SNPs had higher than expected, but not significantly so, spatial variation
484 across scales (all p > 0.05).
485
486 **Discussion**
487
488 The developmental stage at which a plant experiences stress plays a critical role in
489 determining how it responds to that stress (Lawrence-Paul & Lasky, 2024). Our results
490 demonstrate that *when* a plant experiences stress can impact fitness as much as *if* it
491 experiences stress. Developmental phases represent distinct physiological and regulatory
492 states that alter stress resilience, as we found that drought tolerance during the juvenile phase
493 cannot predict tolerance during the adult phase. We present evidence that unique genetic and
494 physiological mechanisms underlie stress resilience across developmental stages, highlighting
495 the importance of studying these phases independently.
496 Further, we observed strong genotype-by-environment interactions, with some
497 genotypes more drought-tolerant in the juvenile phase and others more tolerant in the adult
498 phase. This phase-specific GxE suggests that natural selection can act independently on stress
499 responses at different stages. This GxE and the lack of strong negative correlation between
500 performance under drought at the two different stages (linear regression between fruits
501 produced in juvenile vs adult drought R^2 = 0.1) suggests an opportunity for crop improvement,
502 by selecting for both juvenile and adult-phase drought tolerance traits. In this way, breeders
503 could improve stress resilience across the whole lifespan of a plant. While plant biologists some
504 breeding programs already consider pre and post reproductive traits, our results argue that the
505 two vegetative phases warrant similar attention (Bahuguna *et al.*, 2015; Driedonks *et al.*, 2016;
506 Varoquaux *et al.*, 2019).

507 These findings also caution against relying solely on mutant lines in a single genetic
508 background for studying stress tolerance. Prior studies using miR156 overexpression lines
509 suggest the juvenile phase is more drought-tolerant, however, this was not true for most of the
510 natural accessions examined in this study (Arshad *et al.*, 2017). Accounting for ontogenetic
511 stage in stress experiments could help reconcile inconsistent results across studies and provide
512 a more nuanced understanding of stress biology.

513 We observed considerable natural variation in the timing of VPC among the accessions
514 used in this study. Notably, the duration of each phase; juvenile, adult and reproductive, varied
515 independently, supporting previous findings that VPC and flowering are independently regulated
516 (Zhao *et al.*, 2023). Independent regulation of developmental transitions can allow for
517 developmental phases to align with specific seasonal stress patterns, potentially improving local
518 adaptation. Just as variation in germination and flowering time underlie life history diversity
519 (Korves *et al.*, 2007; Kenney *et al.*, 2014; Burghardt *et al.*, 2015), variation in the timing of VPC
520 may also contribute to different strategies. Previous work links the juvenile phase with fast
521 growth traits like rapid leaf initiation rates, and thin, low-cost tissues, while the adult phase is
522 associated with more expensive tissues with longer lifespans (Lawrence *et al.*, 2022).
523 Therefore, genotypes that remain in the juvenile phase longer may pursue a “fast” life history
524 strategy focused on growth while those that transition earlier to the adult phase may deploy a
525 strategy focused more on survival.

526 We found the timing of VPC was correlated with climate in Iberia, suggesting it plays a
527 role in local adaptation, but otherwise we found evidence that selection may maintain diversity in
528 VPC within most populations of *Arabidopsis*. Specifically, there were very weak correlations
529 between the timing of VPC and global climate variation, and the timing of VPC and drought fruit
530 number GWAS SNPs tended to show very little spatial change in allele frequency (Lasky *et al.*,
531 2024). Thus, tradeoffs associated with variation in the timing of VPC, potentially due to variation

532 in abiotic stress response during the juvenile phase, could reduce fitness effects of VPC and
533 promote diversity locally (Mojica *et al.*, 2012).
534 Together, our findings highlight the critical role of vegetative phase change in shaping
535 stress responses and fitness outcomes. A deeper understanding of ontogenetic shifts in
536 morphology and physiology can help to better understand patterns of local adaptation as well as
537 guide the development of more resilient crops to novel climates.
538
539 **Acknowledgments**
540 This work was supported by NSF IOS-2109780 grant awarded to EHL-P and NIH
541 R35GM138300 grants awarded to JRL.
542
543

544

545 **References**

546 Arshad M, Feyissa BA, Amyot L, Aung B, Hannoufa A. 2017. MicroRNA156 improves drought
547 stress tolerance in alfalfa (*Medicago sativa*) by silencing SPL13. *Plant Science* 258: 122–136.

548 Austen EJ, Rowe L, Stinchcombe JR, Forrest JRK. 2017. Explaining the apparent paradox of
549 persistent selection for early flowering. *New Phytologist* 215: 929–934.

550 Bahuguna RN, Jha J, Pal M, Shah D, Lawas LM, Khetarpal S, Jagadish KSV. 2015.
551 Physiological and biochemical characterization of NERICA-L-44: a novel source of heat
552 tolerance at the vegetative and reproductive stages in rice. *Physiologia Plantarum* 154: 543–
553 559.

554 Bazzaz FA, Chiariello NR, Coley PD, Pitelka LF. 1987. Allocating Resources to Reproduction
555 and Defense. *BioScience* 37: 58–67.

556 Boyes DC, Zayed AM, Ascenzi R, McCaskill AJ, Hoffman NE, Davis KR, Görlach J. 2001.
557 Growth Stage–Based Phenotypic Analysis of Arabidopsis: A Model for High Throughput
558 Functional Genomics in Plants. *The Plant Cell* 13: 1499–1510.

559 Burghardt LT, Metcalf CJE, Wilczek AM, Schmitt J, Donohue K. 2015. Modeling the influence of
560 genetic and environmental variation on the expression of plant life cycles across landscapes.
561 *American Naturalist* 185: 212–227.

562 Donohue K. 2002. GERMINATION TIMING INFLUENCES NATURAL SELECTION ON LIFE-
563 HISTORY CHARACTERS IN ARABIDOPSIS THALIANA. *Ecology* 83: 1006–1016.

564 Doody E, Zha Y, He J, Poethig RS. 2022. The genetic basis of natural variation in the timing of
565 vegetative phase change in Arabidopsis thaliana. *Development* 149.

566 Driedonks N, Rieu I, Vriezen WH. 2016. Breeding for plant heat tolerance at vegetative and
567 reproductive stages. *Plant Reproduction* 29: 67–79.

568 Fick SE, Hijmans RJ. 2017. WorldClim 2: new 1-km spatial resolution climate surfaces for global
569 land areas. *International Journal of Climatology* 37: 4302–4315.

570 Foerster JM, Beissinger T, de Leon N, Kaeppler S. 2015. Large effect QTL explain natural
571 phenotypic variation for the developmental timing of vegetative phase change in maize (*Zea*
572 *mays L.*). *Theoretical and Applied Genetics* 128: 529–538.

573 Franco-Zorrilla JM, Valli A, Todesco M, Mateos I, Puga MI, Rubio-Somoza I, Leyva A, Weigel D,
574 García JA, Paz-Ares J, *et al.* 2007. Target mimicry provides a new mechanism for regulation of
575 microRNA activity. *Nature Genetics* 39: 1033–1037.

576 Gamba D, Lorts CM, Haile A, Sahay S, Lopez L, Xia T, Takou M, Kulesza E, Elango D, Kerby J,
577 *et al.* 2024. The genomics and physiology of abiotic stressors associated with global elevational
578 gradients in Arabidopsis thaliana. *New Phytologist* 244: 2062–2077.

579 Gehan MA, Fahlgren N, Abbasi A, Berry JC, Callen ST, Chavez L, Doust AN, Feldman MJ,
580 Gilbert KB, Hodge JG, *et al.* 2017. PlantCV v2: Image analysis software for high-throughput
581 plant phenotyping. *PeerJ* 5: e4088.

582 He J, Xu M, Willmann MR, McCormick K, Hu T, Yang L, Starker CG, Voytas DF, Meyers BC,
583 Poethig RS. 2018. Threshold-dependent repression of SPL gene expression by miR156/miR157
584 controls vegetative phase change in *Arabidopsis thaliana*. *PLOS Genetics* 14: e1007337.

585 Hudson CJ, Freeman JS, Jones RC, Potts BM, Wong MML, Weller JL, Hecht VFG, Poethig RS,
586 Vaillancourt RE. 2014. Genetic Control of Heterochrony in Eucalyptus globulus. *G3*
587 *Genes|Genomes|Genetics* 4: 1235–1245.

588 Kenney AM, McKay JK, Richards JH, Juenger TE. 2014. Direct and indirect selection on
589 flowering time, water-use efficiency (WUE, δ13C), and WUE plasticity to drought in *Arabidopsis*
590 *thaliana*. *Ecology and Evolution* 4: 4505–4521.

591 Korves TM, Schmid KJ, Caicedo AL, Mays C, Stinchcombe JR, Purugganan MD, Schmitt J.
592 2007. Fitness effects associated with the major flowering time gene FRIGIDA in Arabidopsis
593 thaliana in the field. *The American naturalist* 169.

594 Krysan PJ, Young JC, Sussman MR. 1999. T-DNA as an Insertional Mutagen in Arabidopsis.
595 *The Plant Cell* 11: 2283–2290.

596 Lasky JR, Des Marais DL, Lowry DB, Povolotskaya I, McKay JK, Richards JH, Keitt TH,
597 Juenger TE. 2014. Natural Variation in Abiotic Stress Responsive Gene Expression and Local
598 Adaptation to Climate in Arabidopsis thaliana. *Molecular Biology and Evolution* 31: 2283–2296.

599 Lasky JR, Takou M, Gamba D, Keitt TH. 2024. Estimating scale-specific and localized spatial
600 patterns in allele frequency. *Genetics* 227: iyae082.

601 Lawrence EH, Springer CJ, Helliker BR, Poethig RS. 2022. The carbon economics of vegetative
602 phase change. *Plant Cell and Environment* 45: 1286–1297.

603 Lawrence-Paul E, Lasky J. 2024. Ontogenetic changes in ecophysiology are an understudied
604 yet important component of plant adaptation. *American journal of botany* 111: e16294.

605 Lawrence-Paul EH, Poethig RS, Lasky JR. 2023. Vegetative phase change causes age-
606 dependent changes in phenotypic plasticity. *New Phytologist* 240: 613–625.

607 Lee G, Sanderson, Brian J., Ellis, Thomas J., Dilkes, Brian P., McKay, John K., Ågren, Jon,
608 Oakley, Christopher G. 2024. A large-effect fitness trade-off across environments is explained
609 by a single mutation affecting cold acclimation. *Proceedings of the National Academy of*
610 *Sciences* 121: e2317461121.

611 Lucani CJ, Brodribb TJ, Jordan GJ, Mitchell PJ. 2019. Juvenile and adult leaves of heteroblastic
612 Eucalyptus globulus vary in xylem vulnerability. *Trees* 33: 1167–1178.

613 Lundgren MR, Marais DLD. 2020. Life History Variation as a Model for Understanding Trade-
614 Offs in Plant–Environment Interactions. *Current Biology* 30: R180–R189.

615 Mao H-D, Yu L-J, Li Z-J, Yan Y, Han R, Liu H, Ma M. 2016. Genome-wide analysis of the SPL
616 family transcription factors and their responses to abiotic stresses in maize. *Plant Gene* 6: 1–12.

617 Mojica JP, Lee YW, Willis JH, Kelly JK. 2012. Spatially and temporally varying selection on
618 intrapopulation quantitative trait loci for a life history trade-off in Mimulus guttatus. *Molecular*
619 *Ecology* 21: 3718–3728.

620 R Core Team. 2021. R: A Language and Environment for Statistical Computing.

621 Schindelin J, Arganda-Carreras I, Frise E, Kaynig V, Longair M, Pietzsch T, Preibisch S,
622 Rueden C, Saalfeld S, Schmid B, *et al.* 2012. Fiji: An open-source platform for biological-image
623 analysis. *Nature Methods* 9: 676–682.

624 Telfer A, Bollman KM, Poethig RS. 1997. Phase change and the regulation of trichome
625 distribution in *Arabidopsis thaliana*. *Development* 124: 645–654.

626 Varoquaux N, Cole B, Gao C, Pierroz G, Baker CR, Patel D, Madera M, Jeffers T, Hollingsworth
627 J, Sievert J, *et al.* 2019. Transcriptomic analysis of field-droughted sorghum from seedling to
628 maturity reveals biotic and metabolic responses. *Proceedings of the National Academy of*
629 *Sciences of the United States of America* 116: 27124–27132.

630 Vasseur F, Bresson J, Wang G, Schwab R, Weigel D. 2018. Image-based methods for
631 phenotyping growth dynamics and fitness components in Arabidopsis thaliana. *Plant Methods*
632 14: 1–11.

633 Visentin I, Pagliarani C, Deva E, Caracci A, Turečková V, Novák O, Lovisolo C, Schubert A,
634 Cardinale F. 2020. A novel strigolactone-miR156 module controls stomatal behaviour during
635 drought recovery. *Plant, Cell & Environment* 43vis: 1613–1624.

636 Wang X, Song X, Miao H, Feng S, Wu G. 2024. Natural variation in CYCLIC NUCLEOTIDE-
637 GATED ION CHANNEL 4 reveals a novel role of calcium signaling in vegetative phase change
638 in Arabidopsis. *New Phytologist* 242: 1043–1054.

639 Willmann MR, Poethig RS. 2007. Conservation and evolution of miRNA regulatory programs in
640 plant development. *Current Opinion in Plant Biology* 10: 503–511.

641 Willmann MR, Poethig RS. 2011. The effect of the floral repressor FLC on the timing and
642 progression of vegetative phase change in Arabidopsis. *Development* 138: 677–685.

643 Wu G, Park MY, Conway SR, Wang JW, Weigel D, Poethig RS. 2009. The sequential action of
644 miR156 and miR172 regulates developmental timing in *Arabidopsis*. *Cell* 138: 750–759.

645 Wu G, Poethig RS. 2006. Temporal regulation of shoot development in *Arabidopsis thaliana* by
646 miR156 and its target SPL3. *Development* 133: 3539–3547.

647 Xu M, Hu T, Zhao J, Park M-Y, Earley KW, Wu G, Yang L, Poethig RS. 2016. Developmental
648 functions of miR156-regulated SQUAMOSA PROMOTER BINDING PROTEIN-LIKE (SPL)
649 genes in *Arabidopsis thaliana*. *PLOS Genetics* 12: e1006263.

650 Young TP, Augspurger CK. 1991. Ecology and evolution of long-lived semelparous plants.
651 *Trends in Ecology & Evolution* 6: 285–289.

652 Zhao J, Doody E, Poethig RS. 2023. Reproductive competence is regulated independently of
653 vegetative phase change in Arabidopsis thaliana. *Current Biology* 33: 487–497.

654 Zhao Y, He J, Liu M, Miao J, Ma C, Feng Y, Qian J, Li H, Bi H, Liu W. 2024. The SPL
655 transcription factor TaSPL6 negatively regulates drought stress response in wheat. *Plant*
656 *Physiology and Biochemistry* 206: 108264.

657
658

Supplemental Figures and Tables

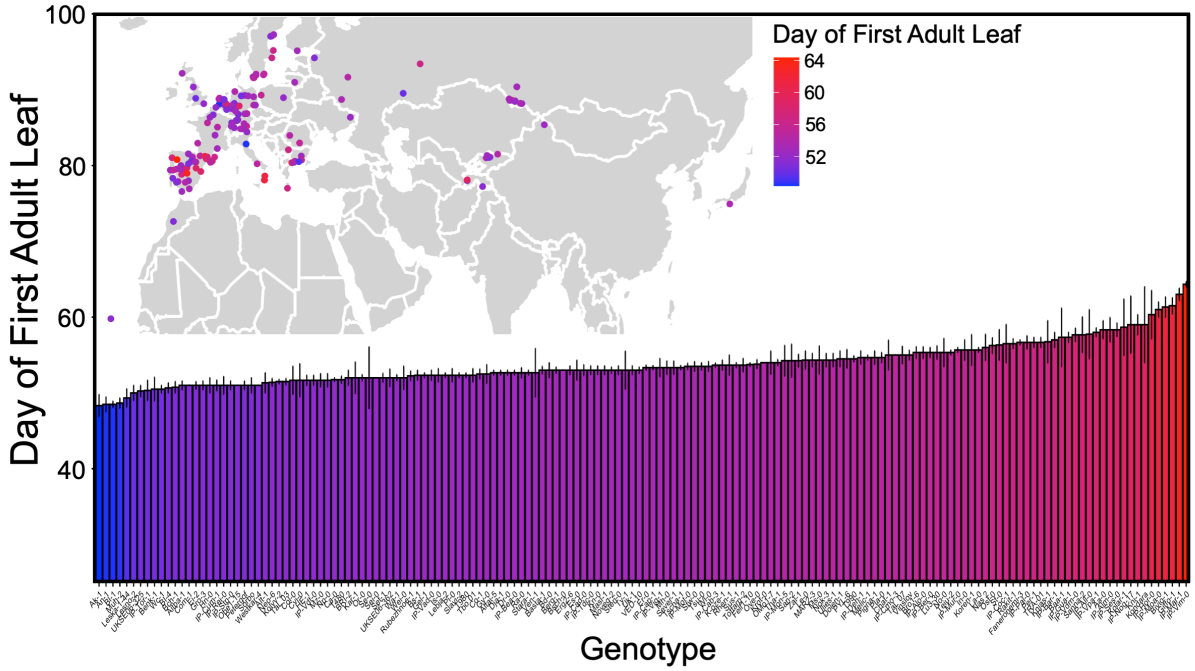

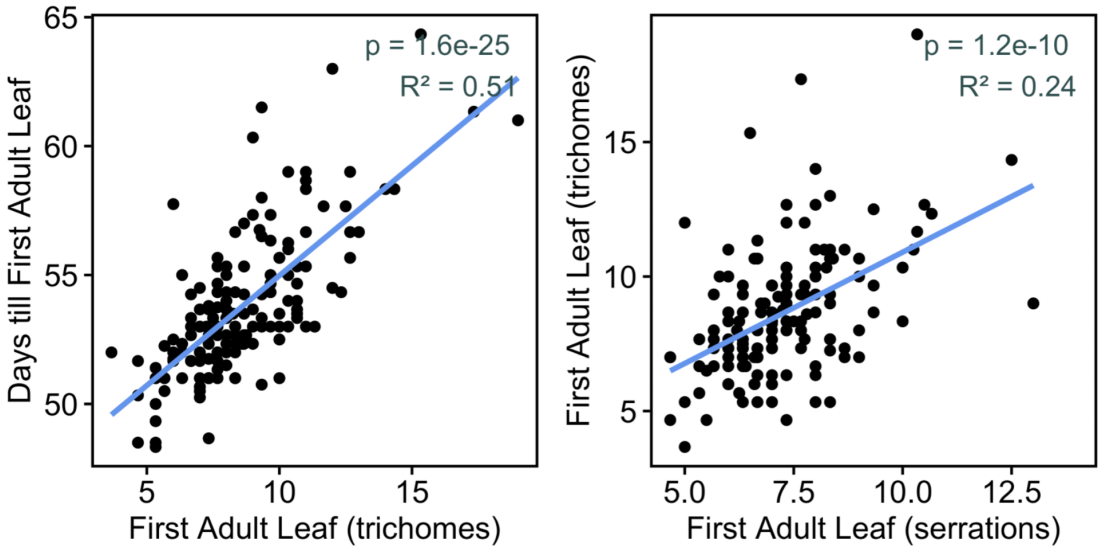

Figure S1. Natural variation in the timing of vegetative phase change (VPC). Timing of VPC based on the days between planting and when the first adult leaf with abaxial trichomes was present for 158 natural accessions used in this study (A). Accessions are plotted on the map in the location where they originated from, and points are colored based on days until the first adult leaf is visible. Bars represent the mean ± SE for a minimum of 3 replicates per genotype. Relationships between the timing of VPC measured as days till the first adult leaf is visible, first adult leaf based on abaxial trichomes and based on serrations (B, C). Results from linear regression analysis displayed in the top right corner of each plot.

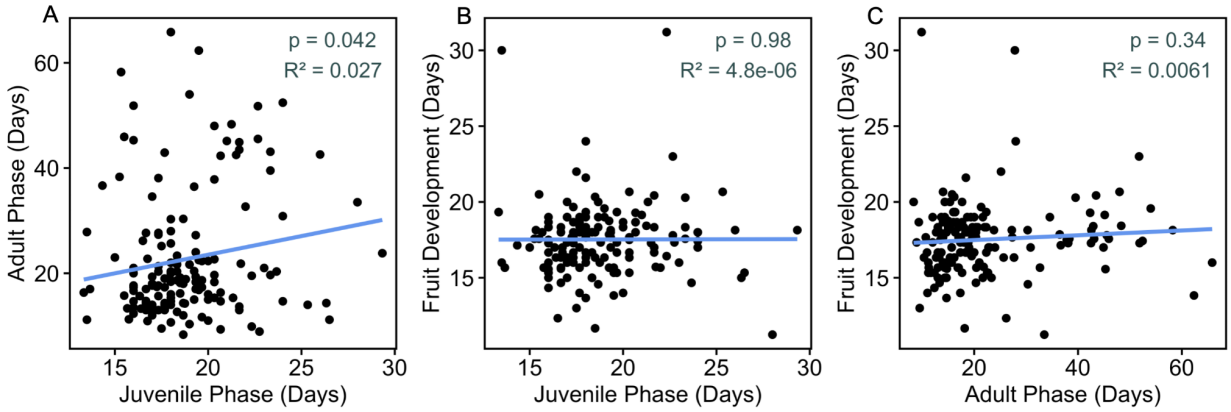

Figure S2. Relationships between time spent in each developmental phase. Juvenile phase is measured as time between planting and first adult leaf present, excluding the 35 days spent at 4℃ for vernalization, adult phase measured as time between first adult leaf present and first open flower, and reproductive phase measured as time between first open flower and first mature fruit. Blue lines represent the line of best fit and results from linear regression analysis displayed in the top right corner of each plot.

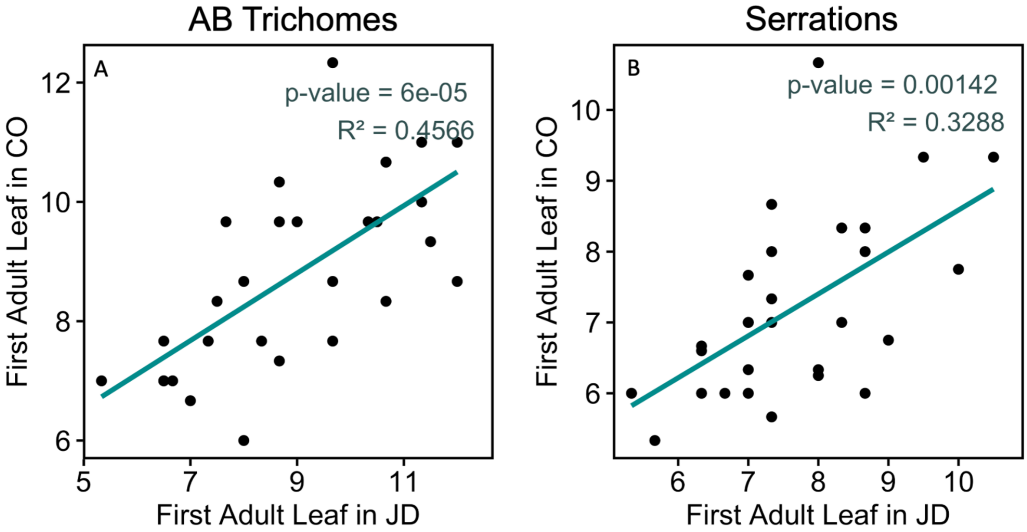

Figure S3. Relationships between the timing of vegetative phase change in well-watered control and juvenile drought treatments based on the first leaf with abaxial trichomes (A) or first leaf with serrations (B). Green lines represent the line of best fit and results from linear regression analysis are displayed in the top right corner of each plot.

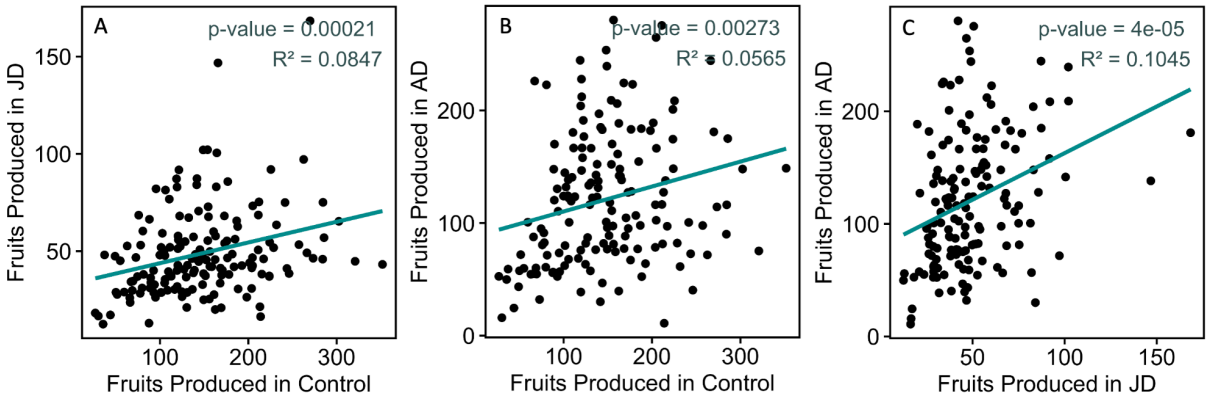

Fig S4. Relationships between the number of fruits produced across well-watered control, juvenile drought (JD) and adult drought (AD) treatments. Green lines represent the line of best fit and results from linear regression analysis are displayed in the top right corner of each plot.

Table S1: *Arabidopsis thaliana* accessions used in this study including ABRC stock ID, 1001 genomes project accession ID, location information and group for timing of droughts in experiment.

ExpID	Genotype	StockID	1001g_ID	Country	Latitude	Longitude	Drought_Group
1	Col-0	CS70000	6909	USA	38.3	-92.3	2
2	miR156OX	NA	NA	NA	NA	NA	2
3	MIM156	NA	NA	NA	NA	NA	2
4	Co-1	CS76468	7077	POR	40.12	-8.25	1
5	Cvi-0	CS76789	6911	CPV	15.1111	-23.6167	1
6	Fell1-10	CS76855	9814	GER	48.42	8.79	2
7	IP-All-0	CS76659	9517	ESP	42.19	-7.8	1
9	IP-Gua-1	CS76894	9544	ESP	39.4	-5.33	2
10	IP-Mot-0	CS77109	9560	ESP	38.19	-6.24	1
12	Is-0	CS78904	8312	GER	50.5	7.5	2
13	Kar-1	CS76522	763	KGZ	42.3	74.3667	1
14	Kn-0	CS76969	7186	LTU	54.8969	23.8924	1
15	Neo-6	CS76560	772	TJK	37.35	72.4667	1
16	Np-0	CS76563	7268	GER	52.6969	10.981	1
17	Or-0	CS76568	7282	GER	50.3827	8.01161	1
18	Per-1	CS76571	8354	RUS	58	56.3167	2
19	Ra-0	CS76582	6958	FRA	46	3.3	1
20	Sei-0	CS76599	7333	ITA	46.5438	11.5614	1
21	Stw-0	CS76605	7347	RUS	52	36	2
22	Sus-1	CS76607	765	KGZ	42.1833	73.4	1
23	TaL 07	CS77339	6180	SWE	62.6322	17.6906	1
24	VED-10	CS78839	9933	FRA	43.74	3.89	1
25	Westkar-4	CS76629	9766	KGZ	42.26	74.16	1
26	Aitba-1	CS76649	9606	MAR	31.48	-7.45	1
27	Alt-1	CS76663	9774	GER	48.59	9.22	1
28	An-1	CS76435	6898	BEL	51.2167	4.4	1
29	Lu3-30	CS77057	9782	GER	48.53	9.09	3
30	Melic-1	CS77078	9657	ITA	38.45	16.04	1
31	Muh-2	CS77113	9803	GER	48.42	8.76	1
32	Mz-0	CS76557	6940	GER	50.3	8.3	1
33	PYL-6	CS77198	265	FRA	44.65	-1.16667	2
34	Sorbo	CS78917	6963	TJK	38.35	68.48	2
35	Bch-1	CS76444	7028	GER	49.5166	9.3166	1
37	Giffo-1	CS76878	9653	ITA	38.44	16.13	3
38	In-0	CS78903	8311	AUT	47.5	11.5	2
39	IP-Vig-1	CS78843	9597	ESP	42.31	-2.53	3
40	Ove-0	CS76569	7287	GER	53.3422	8.42255	2
41	Petergof	CS77170	7296	RUS	59	29	2
42	Set-1	CS78787	5772	UK	54.1	-2.3	2
43	Sten-0	CS77277	7346	GER	52.6058	11.8558	3
44	Dja-1	CS76473	766	KGZ	42.5833	73.6333	1
45	Hn-0	CS76513	7165	GER	51.3472	8.28844	2
46	IP-Vad-0	CS78826	9591	ESP	42.86	-3.59	3

48	Mh-0	CS76550	7255	POL	50.95	7.5	1
49	Pi-0	CS76572	7298	AUT	47.04	10.51	3
50	Ty-1	CS78790	5784	UK	56.4	-5.2	3
51	Wei-0	CS76628	6979	SUI	47.25	8.26	1
52	Berg-1	CS76701	9775	GER	48.41	8.79	2
53	Ca-0	CS76459	7062	GER	50.2981	8.26607	1
54	Le-0	CS76540	7218	NED	52.1611	4.49015	2
55	St-0	CS77270	8387	SWE	59	18	2
56	Erg2-6	CS76845	9784	GER	48.5	8.8	2
57	IP-Bea-0	CS76695	9522	ESP	36.52	-5.27	2
58	IP-Cab-3	CS76738	9526	ESP	41.54	2.39	2
59	IP-Cmo-3	CS76774	9534	ESP	40.05	-4.65	2
60	Se-0	CS76597	6961	ESP	38.3333	-3.53333	1
61	Tsu-0	CS77389	7373	JPN	34.43	136.31	3
62	Ak-1	CS76431	6987	GER	48.0683	7.62551	1
63	BI-4	CS76706	9813	GER	48.4	8.77	1
64	Bsch-0	CS76457	7031	GER	50.0167	8.6667	3
65	HE-1	CS76916	9769	GER	48.55	8.99	1
66	IP-Cum-1	CS76787	9537	ESP	38.07	-6.66	1
67	IP-Rei-0	CS77208	9510	POR	38.75	-7.59	2
68	MAR2-3	CS77070	159	FRA	47.35	3.93333	3
69	Obe1-15	CS77139	9804	GER	48.45	8.87	2
70	Pigna-1	CS77177	9659	ITA	41.18	14.18	2
71	Wc-1	CS76627	7404	GER	52.6	10.0667	1
72	Zal-1	CS76634	768	KGZ	42.8	76.35	3
74	Wa-1	CS76626	7394	POL	52.3	21	2
75	IP-Deh-1	CS76793	9539	ESP	40.29	-6.67	3
76	Bs-1	CS78888	7003	SUI	47.5	7.5	2
77	Chat-1	CS76463	7071	FRA	48.0717	1.33867	2
78	IP-Alo-0	CS76662	9506	POR	40.11	-7.47	3
79	IP-Mon-5	CS77107	9559	ESP	38.06	-4.38	2
80	IP-Vim-0	CS78844	9598	ESP	41.88	-6.51	4
82	Knjas-1	CS76971	9749	SRB	43.54	22.29	4
83	Kolar-1	CS76974	9699	BUL	41.37	23.14	3
84	Rubezhnoe-1	CS76594	7323	UKR	49	38.28	2
85	T480	CS77300	6108	SWE	55.7989	13.1206	3
86	No-0	CS77128	7273	GER	51.0581	13.2995	2
87	Uk-1	CS76620	7378	GER	48.0333	7.7667	2
88	Com-1	CS76469	7092	FRA	49.416	2.823	1
89	Gel-1	CS76492	7143	NED	51.0167	5.86667	1

90	Krot-0	CS76534	7203	GER	49.631	11.5722	1
91	La-0	CS76538	7209	POL	52.7333	15.2333	1
92	Stara-1	CS77271	9713	BUL	42.49	25.61	2
93	Altai-5	CS76433	9758	CHN	47.75	88.4	1
95	Dr-0	CS78897	7106	GER	51.051	13.7336	1
96	Faneronemi-3	CS76853	9726	GRC	37.07	22.04	2
97	IP-Cap-1	CS76741	9529	ESP	36.97	-3.36	3
98	IP-Hor-0	CS76930	9547	ESP	41.67	2.62	3
100	IP-Ses-0	CS77244	9582	ESP	41.48	-1.63	4
101	IP-Vdt-0	CS78838	9595	ESP	40.89	-5.5	3
102	IP-Vpa-1	CS78850	9602	ESP	40.5	-3.96	3
103	Lesno-2	CS77033	9612	RUS	53.04	51.94	3
105	Noveg-2	CS77132	9637	RUS	51.77	80.85	3
107	Sever-1	CS77245	9643	RUS	52.1	79.31	3
108	Slavi-2	CS77252	9723	BUL	41.42	23.67	3
110	Vinslov	CS78847	9057	SWE	56.1	13.9167	3
111	Wl-0	CS76630	7411	GER	47.9299	10.8134	2
112	Baa-1	CS76442	7002	NED	51.3333	6.1	4
113	Bivio-1	CS76713	9649	ITA	39.13	16.17	3
114	IP-Alm-0	CS76660	9518	ESP	39.88	-0.36	4
115	IP-Bar-1	CS76689	9521	ESP	41.43	2.13	4
116	IP-Cad-0	CS76739	9527	ESP	40.37	-5.74	3
118	Koren-1	CS76983	9719	BUL	41.83	25.69	3
119	Tscha-1	CS76616	7372	AUT	47.0748	9.9042	3
124	San-2	CS77233	8247	SWE	56.07	13.74	4
125	Rakit-1	CS77202	9640	RUS	51.87	80.06	4
126	Aa-0	CS76428	7000	GER	50.9167	9.57073	3
127	BRI-2	CS76725	9910	FRA	50.68	3.52	2
128	Dolen-1	CS76802	9697	BUL	41.62	23.94	3
129	IP-Mar-1	CS77068	9555	ESP	39.58	-3.93	4
130	IP-Mur-0	CS77115	9562	ESP	41.67	2	4
131	Kni-1	CS76970	6040	SWE	55.66	13.4	4
132	Kolyv-2	CS76977	9625	RUS	51.31	82.59	3
133	Kondara	CS76532	6929	TJK	38.48	68.49	3
134	Rhen-1	CS78916	7316	NED	51.9667	5.56667	4
135	UKSE06-362	CS78802	5165	UK	51.3	0.4	4
136	Bd-0	CS76445	7013	GER	52.4584	13.287	1
137	IP-Ber-0	CS78887	9524	ESP	42.52	-0.56	4
138	IP-Pal-0	CS77159	9567	ESP	42.34	1.3	4
139	K-oze-1	CS76957	9629	RUS	51.35	82.18	2

140	Leska-1-44	CS77030	9716	BUL	41.54	24.98	4
141	Nok-3	CS76562	6945	NED	52.24	4.45	4
143	Pla-0	CS76573	8357	ESP	41.5	2.25	3
144	Teiu-2	CS77361	9736	ROU	44.69	25.17	3
146	IP-Moa-0	CS77102	9557	ESP	42.46	0.7	4
148	IP-Tor-1	CS77378	9589	ESP	41.6	-2.83	4
149	Ms-0	CS76555	6938	RUS	55.7522	37.6322	3
150	Tha-1	CS76611	7353	NED	52.08	4.3	3
151	Ulies-1	CS78815	9737	ROU	45.95	22.62	3
152	Masl-1	CS77073	9634	RUS	54.13	81.31	4
153	Basta-1	CS76691	9619	RUS	51.84	79.48	2
154	Bl-1	CS76450	7025	ITA	44.5041	11.3396	2
155	Ei-2	CS76478	6915	GER	50.3	6.3	2
156	Gy-0	CS78901	8214	FRA	49	2	3
158	IP-Stp-0	CS77283	9584	ESP	41.19	-3.58	4
160	Lebja-2	CS77016	9632	RUS	51.67	80.82	3
161	OMo1-7	CS77147	6073	SWE	56.1481	15.8155	4
162	Ost-0	CS77154	8351	SWE	60.25	18.37	4
163	T980	CS77327	6150	SWE	55.9261	13.5319	4
164	TaL 03	CS77338	6177	SWE	62.6322	17.69	4
166	Tottarp-2	CS77381	6243	SWE	56.27373	13.90045	1
167	TRA-01	CS77384	6244	SWE	62.9169	18.4728	4
168	Ven-1	CS76624	7384	NED	52.0333	5.55	4
169	Es-0	CS76484	7126	FIN	60.1997	24.5682	4
170	Er-0	CS78898	7125	GER	49.5955	11.0087	3
171	Nas 2	CS77122	9427	SWE	62.8815	18.4055	4
172	Sanna-2	CS77234	8376	SWE	62.69	18	4
173	IP-Nog-17	CS77129	9564	ESP	40.45	-1.6	4
174	IP-Vdm-0	CS78837	9594	ESP	42.04	1.01	4
176	T990	CS77328	6151	SWE	55.6528	13.2244	4
177	UKSE06-325	CS78801	5151	UK	52.2	-1.7	4
178	Gro-3	CS76889	6025	SWE	62.6437	17.7339	4
186	IP-Tdc-0	CS77344	9587	ESP	41.5	-1.88	4
187	Bro1-6	CS76726	8231	SWE	56.3	16	4
188	Tbo 01	CS77343	6184	SWE	62.8892	18.4522	4
190	IP-Coc-1	CS76776	9535	ESP	42.31	3.19	4
192	Benk-1	CS76447	7008	NED	52	5.675	4